# Formation of Surface Traps on Quantum Dots by Bidentate Chelation and Their Application in Low-Potential Electrochemiluminescent Biosensing

## Xuan Liu, Lingxiao Cheng, Jianping Lei, Hui Liu, and Huangxian Ju*[a]

**Abstract:** Bidentate chelation, *meso*-2,3-dimercaptosuccinic acid (DMSA), was used as a stabilizer for the synthesis of CdTe quantum dots (QDs). The bidentate chelate QDs, characterized with FT-IR, PL, and UV/Vis spectroscopy; element analysis; and high-resolution transmission electron microscope, exhibited surface traps due to the large surface/volume ratio of QD particle and the steric hindrance of the DMSA molecule. The unpassivated surface of the QDs produced a narrower band gap than the core and electrochemiluminescent (ECL) emission at relatively low cathodic potential. In air-saturated pH 7.0 buffer, the QDs immobilized on electrode surface showed an intense ECL emission peak at −0.85 V (vs. Ag/AgCl). $H_2O_2$ produced from electrochemical reduction of dissolved oxygen was demonstrated to be the co-reactant, which avoided the need of strong oxidant as the co-reactant and produced a sensitive analytical method for peroxidase-related analytes. Using hydroquinone/horseradish peroxidase/$H_2O_2$ as a model system, a new, reagentless, phenolic, ECL biosensor for hydroquinone was constructed, based on the quenching effect of ECL emission of QDs by consumption of co-reactant $H_2O_2$. The biosensor showed a linear range of 0.2–10 μM with acceptable stability and reproducibility. This work opens new avenues in the search for new ECL emitters with excellent analytical performance and makes QDs a more attractive alternative in biosensing.

**Keywords:** biosensors · cadmium · electrochemiluminescence · luminescence · tellurium · quantum dots

## Introduction

Electrochemiluminescence (ECL) is a fascinating phenomenon, due to its promising application in many fields.[1,2] A number of new ECL-emitting species with high ECL efficiency have gradually been synthesized[3,4] and used to label biomolecules for fundamental study and for analytical applications.[2] The majority of ECL-emitting species employed in bioanalysis are derived from [Ru(bpy)$_3$]$^{2+}$.[5–7] Recently, quantum dots (QDs) have attracted considerable interest in ECL analysis,[8–10] since the ECL behavior of Si QDs in organic solvent was reported.[11] Compared with Ru compounds, the ECL of QDs possesses many advantages, such as neutral detection conditions and the easy realizability in both cathodic and anodic processes with diverse co-reactants,[12–14] leading to multifarious biosensing strategies. The first QD-ECL biosensor for glucose was based on the cathodic ECL quenching by an enzymatic reaction to transform an efficient co-reactant into another less effecient co-reactant.[15] A signal on a CdS QD-ECL biosensor for choline and acetylcholine was then probed by ECL response with the co-reactant formed from bi-enzymatic cycles.[8] In addition, anodic ECL bioanalysis methodologies have also been developed for the detection of dopamine and tyrosine with high sensitivity.[10,14] However, most of the reported QD-based ECL systems need a relatively high applied potential, which is unfavorable to elimination of undesirable reactions[16] and has slowed the development of QD-based ECL biosensing technology. Thus, the current research challenge is to develop new QD-ECL biosensors with the low applied potential and highly efficient ECL emission.

Great efforts have focused on reducing the ECL applied potential of QDs, such as using carbon nanotubes to accelerate the electron transfer between QDs and the electrode,[8] employing different materials as working electrode[10] and changing the components of detection solution.[17] However, the achieved progress is rather limited. To further decrease

[a] X. Liu, L. Cheng, Dr. J.-P. Lei, H. Liu, Prof. H.-X. Ju
MOE Key Laboratory of Analytical Chemistry for Life Science
School of Chemistry and Chemical Engineering
Nanjing University, Nanjing 210093 (P. R. China)
Fax: (+86)25-8359-3593
E-mail: hxju@nju.edu.cn

the ECL emission potential, starting from the fundamentals of the ECL process is more effective. Different from photoluminescent (PL) emission,[18–22] which is dominated by excitation within the core of QDs, the ECL emission is characteristic of surface energy levels, because the electron transfer occurs at the surface of the QDs.[2,23] The surface states generally have a much narrower band gap than the core.[11,23] Thus a common feature of ECL behavior obtained from surface traps of unpassivated QDs is the considerable red-shifted ECL by hundreds of nanometers with respect to their PL.[11] Meanwhile, the reduction potential of the QDs shifts to a more positive value with the decreasing band gap.[24] This leads to an approach to obtain a low ECL emission potential in an aqueous system by designing unpassivated surfaces of water-soluble QDs.

The surface/volume ratio is an important factor for surface passivation.[23] The above-mentioned QDs are slightly larger than 2.5 nm and have relatively small surface/volume ratio, which leads to better passivation of a QD surface. In this work we report for the first time on the design of unpassivated QD surfaces by using a short chain dithiol compound, *meso*-2,3-dimercaptosuccinic acid (DMSA), as stabilizer and a Te electrode as Te source.[25] The rigid structure and steric hindrance of DMSA molecule inhibited the growth of crystals and their linkage to the QD surface led to an unpassivated surface with low-potential ECL emission. The co-reactant of the ECL emission was produced from the reduction of dissolved oxygen, which avoided the presence of a strong oxidant. By co-immobilizing QDs and horseradish peroxidase (HRP) on a glassy carbon electrode (GCE), an ECL biosensor for hydroquinone (HQ) was constructed. This work provides a new strategy for designing ECL emitters with excellent analytical performance and extended the application of QDs in bioanalysis.

## Results and Discussion

**Characterization of DMSA–CdTe QDs**: The formation of DMSA–CdTe QDs was confirmed by the FT-IR spectra. The QD powder acquired by centrifugation of a solution of the QDs was used in this experiment. Comparing with DMSA (Figure 1, curve a), the FT-IR spectrum of DMSA–CdTe QDs (Figure 1, curve b) did not show the stretch vibration peaks of S−H bond at 2566.3 and 2533.4 $cm^{-1}$, indicating the formation of S−Cd bonds between DMSA and CdTe core. In addition, the asymmetric vibration peak of carboxyl group also shifted from 1693.6 (curve a) to 1614.2 $cm^{-1}$ (curve b), which could be attributed to the transformation of the −COOH group in DMSA to its anion during the synthesis of the QDs. These results confirmed that the two S−H groups of DMSA molecule were bound to $Cd^{2+}$ to form bidentate chelate QDs with a stable structure.[26]

The X-ray photoelectron spectroscopic (XPS) data showed a molar Cd/Te/S ratio of 116.9:1:85.44 on the surface of the as-prepared QDs, indicating an extremely low Te con-
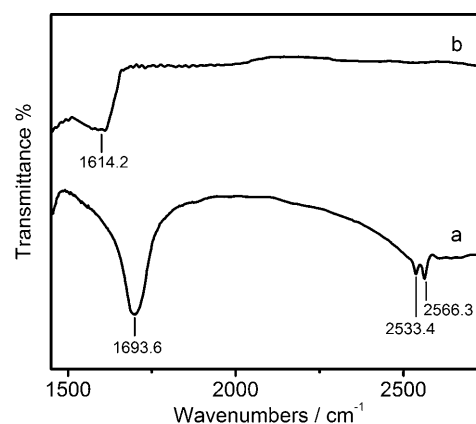


Figure 1. FT-IR spectra of DMSA (curve a) and DMSA–CdTe QDs powder (curve b).

tent on the QD surface. The Cd and DMSA were stable against $O_2$, resulting in a stable QD structure.[27]

Figure 2 shows the UV/Vis spectrum of DMSA–CdTe QDs. An absorption inflection point at 465 nm is defined as peak value to produce a diameter of 1.1 nm calculated ac-
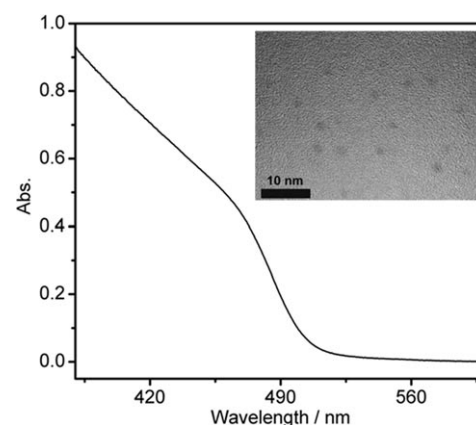


Figure 2. UV/Vis spectrum and HRTEM image (inset) of the DMSA–CdTe QDs.

cording to Peng's empirical equation,[28] indicating an ultrasmall particle size compared to the QD particles reported previously.[8,9,29,30] This result is consistent with the observation from the high-resolution transmission electron microscopic (HRTEM) image, in which a uniform size distribution of about 1.5 nm in diameter is observed (inset in Figure 2). For nanoparticles, small size means large surface/volume ratio, which is beneficial in order to obtain unpassivated surfaces. In addition, the inconspicuous extinction absorption peak of the QDs can be attributed to the surface traps on the QD particles, which is similar to the phenomenon observed previously.[31]

The PL spectrum of the as-prepared QDs also confirmed the existence of surface traps. Different from the monothiol-stabilized CdTe QDs,[10,25] the PL spectrum of DMSA–CdTe QDs showed two PL peaks at 462 and 616 nm (Figure 3,
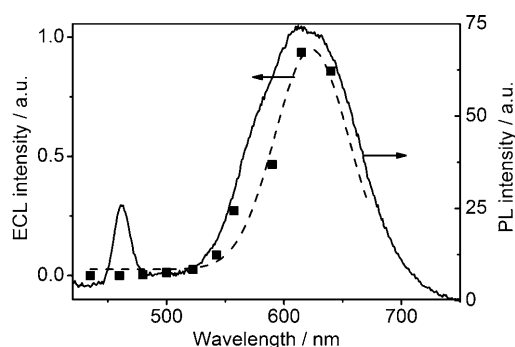
Figure 3. PL (solid line, $\lambda_{ex}$: 400 nm) and ECL (dashed line, at −0.85 V) spectra of the DMSA–CdTe QDs.

solid curve), respectively. The peak position of 462 nm with weaker emission was coincident with the first absorption range of UV/Vis spectrum, indicating that the PL emission came from the core.[31] The wavelength difference between the main PL emission peak at 616 nm and the first absorption peak was 151 nm, which was much greater than those of general surface-passivated CdTe QDs,[10,25] indicating the PL peak at 616 nm was due to the surface trap emission of surface-unpassivated QDs.[11,31] The PL emission intensities at both 616 and 462 nm were relatively low, which was also attributed to the unpassivated surface.[23] The trap emission provided a possibility to obtain a low ECL emission potential.

**Element analysis of the QDs samples**: Monothiol-stabilized mercaptopropionic acid (MPA)–CdTe QDs were selected as surface passivated QDs for comparison; these QDs were prepared with the same procedure and showed a size of 3.4 nm (calculated from Peng's empirical equation[28]). The smaller size of DMSA–CdTe QDs than MPA–CdTe QDs could be attributed to the stronger binding of DMSA to the CdTe surface, which inhibited the growth of crystal. Before elemental analysis, the resulting solutions of QDs were first-ly centrifuged, and the precipitates were washed twice by using 1:1 (v/v) mixture of deionized water and isopropyl alcohol to remove the excess stabilizers. The precipitates were then thoroughly dried and the elemental analysis detection was carried out.

From the carbon compositions of 2.35 and 8.67 % and the ratios of C to S in the two kinds of QDs, the sulfur compositions in DMSA–CdTe QDs and MPA–CdTe QDs were cal-culated to be 3.13 and 7.71 %, respectively. Considering the 2.27 times larger surface/volume ratio (calculated from the diameters of QD particles) and 2.46 times smaller sulfur composition of DMSA–CdTe QDs than the surface-passivat-ed MPA-CdTe QDs, the ratio of coverages of DMSA to MPA on the QD particle surface was determined to be 1:11.17. Thus DMSA–CdTe QDs should have a larger amount of surface traps, even if the tellurium surface sites could be more easily passivated by a surrounding compo-nent.[32] The surface traps result for three reasons. Firstly, the large surface/volume ratio is detrimental for surface pas-

sivation.[23] Secondly, the steric hindrance of the DMSA molecule is larger than that of MPA molecule owing to the two *cis*-carboxyl groups, which resisted the linkage of stabil-izer DMSA to the QD surface. Thirdly, the large surface curvature resulting from the small particle size makes the ar-rangement of dithiol stabilizer on the surface more difficult, thus producing an unpassivated surface.

**ECL and electrochemical behaviors of the surface unpassi-vated QDs**: After the surface-unpassivated QDs were im-mobilized on a glassy carbon electrode (GCE) and covered with chitosan, the cathodic scan from 0 to −0.90 V in air-sa-turated pH 7.0 Tris-HCl buffer (detection solution) pro-duced an ECL emission with a peak potential of around −0.85 V and an onset of −0.59 V (vs. Ag/AgCl; Figure 4,
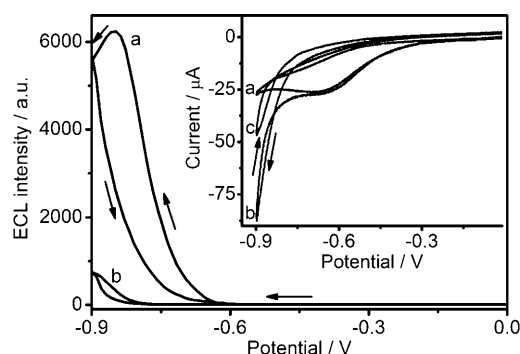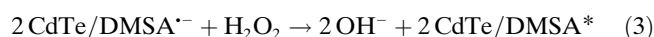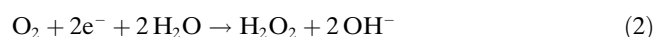


Figure 4. Cyclic ECL curves of GCE/QDs/chitosan in a) air-saturated and b) air-free detection solutions. Inset: Cyclic voltammetry curves of a) chi-tosan-modified GCE and b) GCE/QDs/chitosan in air-saturated detec-tion solution and c) GCE/QDs/chitosan in air-free detection solution.

curve a). This cathodic emission potential was the most posi-tive potential compared to those reported previously for cathodic ECL of QDs by using saturated Ag/AgCl[8–9,15] or calomel[12] as reference electrodes, except one observed for an aqueous solution of CdTe QDs.[25] In addtion, the ECL emission intensity was acceptable when compared with the traditional QD-ECL systems.[8,12] This intensive ECL emis-sion relied on the concentration of dissolved $O_2$, and de-creased by a large degree in an air-free detection solution (Figure 4, curve b). Moreover, the ECL spectrum showed a peak at 623 nm (Figure 3, dashed line), which was consistent with the surface trap emission peak of PL spectrum at 616 nm. Thus, the ECL emission should originate from the surface traps, not from band gap of the core. Also, this phe-nomenon could be attributed to the much narrower band gap of unpassivated surface states than the core.[11,23]

In an air-saturated detection solution, both the chitosan- (inset in Figure 4, curve a) and QD/chitosan-modified (inset in Figure 4, curve b) GCEs showed a reduction peak at −0.64 V with the same peak current, while this peak disap-peared after degassed (inset in Figure 4, curve c). Thus this peak could be attributed to the reduction of dissolved $O_2$. Furthermore, dissolved $O_2$ could maintain good penetration

ability in both chitosan and QD/chitosan film. At such a potential, $O_2$ could be reduced to produce $H_2O_2$,[33] which has been extensively used as a co-reactant of cathodic ECL of QDs.[8,9] With the further cathodic scan the cathodic curves of GCE/QDs/chitosan in both air-saturated and air-free detection solutions showed an increasing current, which was different from the chitosan-modified GCE due to the reduction of QDs (inset in Figure 4). The reduction potential corresponded to the ECL emission potential of the surface-unpassivated QDs, and was much more positive than those reported previously for reduction of QDs, indicating the reduction of surface traps.

Upon addition of 1 mm $H_2O_2$ in air-free detection solution, the GCE/QDs/chitosan showed a strong ECL emission. After $H_2O_2$ was added in air-saturated detection solution, the ECL emission was also increased. Thus the co-reactant of this ECL emission process was $H_2O_2$, which was produced from the dissolved $O_2$ reduction at $-0.64$ V and reacted with the electron injected QDs, providing an ECL system much milder for bioanalysis without the presence of strong oxidants as co-reactant. The ECL process could be expressed as follows [Eqs. (1)–(3)].

$$CdTe/DMSA + e^- \rightarrow CdTe/DMSA^{\cdot-} \quad (1)$$

$$O_2 + 2e^- + 2H_2O \rightarrow H_2O_2 + 2OH^- \quad (2)$$

$$2CdTe/DMSA^{\cdot-} + H_2O_2 \rightarrow 2OH^- + 2CdTe/DMSA^* \quad (3)$$

Simultaneously, trace $O_2$ remained at unreduced state in the QD film might directly react with CdTe/DMSA$^{\cdot-}$ to produce CdTe/DMSA* [Eq. (4)]; the produced CdTe/DMSA* would then gave out light emission [Eq. (5)]

$$2CdTe/DMSA^{\cdot-} + O_2 + 2H^+ \rightarrow 2CdTe/DMSA^* + H_2O_2 \quad (4)$$

$$CdTe/DMSA^* \rightarrow CdTe/DMSA + h\nu \quad (5)$$
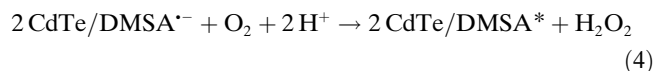
**Quenching effect of ECL emission on the GCE/QDs/HRP–chitosan biosensor**: As $H_2O_2$ is a substrate of multifarious enzymatic reactions based on peroxidases, through immobilization of different peroxidases on the QD/GCE system and the combination of $H_2O_2$-related enzymatic reactions, plenty of biosensors for peroxidase-related analytes could be developed. To verify the application of the surface-unpassivated QDs in biosensing, we used HRP as a model enzyme and HQ as its substrate to construct a new reagentless phenolic ECL biosensor. After HRP was assembled on the QD/GCE surface, the cathodic scan in air-saturated detection solution in presence of HQ would produce an enzymatic reaction as expressed in Equation (6). Consequentially, the consumption of co-reactant $H_2O_2$ for HQ oxidation could weaken the process expressed in Equations (3) and (4), causing the decrease of ECL intensity (Figure 5 A).
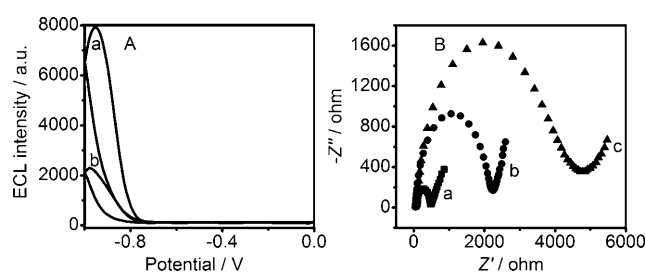
$$HQ + H_2O_2 \rightarrow Quinone + H_2O \quad (6)$$



Figure 5. A) Cyclic ECL curves of GCE/QDs/HRP–chitosan in air-saturated detection solution containing a) 0 and b) 5 μM HQ. B) Nyquist diagrams of electrochemical impedance spectra of a) bare GCE, b) GCE/QDs/chitosan, and c) GCE/QDs/HRP–chitosan in 0.1 M KCl containing 5 mM $[Fe(CN)_6]^{3-}$ and 5 mM $[Fe(CN)_6]^{4-}$.

The applied potential of GCE/QDs/HRP–chitosan was between 0 and $-1.0$ V, while the narrowest potential range applied for ECL biosensing of QDs reported previously were generally wider than 0 to $-1.35$ V.[8–9,12,15,34] The ECL peak potential of the biosensor was at $-0.95$ V, which was 100 mV more negative than that of GCE/QDs/chitosan. This was due to the larger impedance of GCE/QDs/HRP–chitosan than GCE/QDs/chitosan (Figure 5 B).

In the air-saturated detection solution, HQ showed a quenching effect on the ECL emission of GCE/QDs/HRP–chitosan. Further, from the results shown in Figure 6, HQ
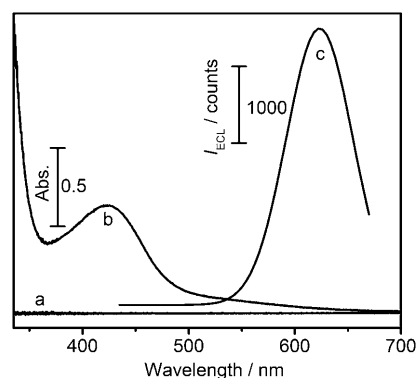


Figure 6. UV/Vis spectra of a) HQ and b) quinone and c) ECL spectrum of GCE/QDs/chitosan in air-saturated detection solution.

did not show any absorption in the studied wavelength range (curve a), and its oxidation state (i.e., as quinone) in presence of HRP and $H_2O_2$, showed an absorption peak at 422 nm (curve b), while the ECL peak of the DMSA–CdTe QDs occurred at 623 nm (curve c), consistent with the PL spectrum. Thus, HQ itself and quinone could not be the acceptor of energy from the excited state of the DMSA–CdTe QDs, and the energy transfer from the excited state of the DMSA–CdTe QDs to HQ and quinone could be excluded. In addition, the amount of quinone at the electrode surface was extremely small at $-0.95$ V, and did not affect the ECL quenching. Alternatively, the ECL quenching should result

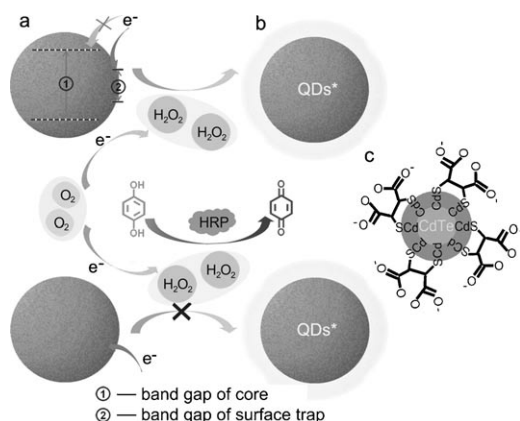from the consumption of $H_2O_2$ at the surface of the biosensor as shown in Figure 7.



Figure 7. Cathodic ECL mechanism of GCE/QDs/chitosan and biosensing mechanism of the biosensor for HQ. a) Electron injection to surface trap of QDs, b) ECL emission from excited QDs*, and c) chemical banding structure of QDs. The quenching results from the consumption of $H_2O_2$ formed during the cathodic scan.

**HQ detection**: Upon addition of HQ in an air-saturated detection solution, the ECL emission of GCE/QDs/HRP–chitosan decreased greatly, and a linear calibration plot of $I_0/I$ value versus HQ concentration could thus be obtained in the concentration range of 0.2 to 10 μM, for which $I_0$ and $I$ are the maximum ECL intensities in absence and presence of HQ at the respective concentration, respectively. The linear regression equation was $I_0/I = 1.03 + 0.708$ [HQ] (concentration in μM; $R = 0.998$, $n = 12$). The detection limit at a signal-to-noise ratio of 3 was 24.7 nM. The detection range was acceptable when compared with the proposed electrochemical and PL sensors,[35,36] especially better than these electrochemical sensors based on the catalysis of HRP.[37–39]

The quenching efficiencies of several phenolic compounds to the ECL emission of GCE/QDs/HRP–chitosan were listed in Table 1. HQ showed the largest quenching efficiency, and only HQ showed a linear response, which was attributed to a variety of enzymatic reactions as reported in previous report.[40]

Table 1. Responses of 5 μM of multifarious phenolic compounds on GCE/QDs/HRP–chitosan in an air-saturated pH 7.0 Tris-HCl buffer solution.

| | HQ | Phenol | Catechol | Resorcinol | *m*-Cresol | *p*-Cresol |
|---|---|---|---|---|---|---|
| response (normalized) | 1 | 0.57 | 0.33 | 0.35 | 0.30 | 0.18 |

**Interference investigation**: To evaluate the selectivity of the present biosensing system, the effects of nine common compounds as foreign species on HQ detection with this ECL biosensor were examined. 10 μM of potassium chloride, po-

tassium nitrate, sodium fluoride, zinc acetate, potassium iodide, ferrous sulphate, ascorbic acid (AA), uric acid (UA) and potassium perchlorate were individually added into the air-saturated detection solution containing 5 μM HQ. As shown in Figure 8, most of the compounds had no interfering effect on HQ detection except $Zn(Ac)_2$ and AA, which slightly decreased the ECL intensity by 11.7 and 12.8 % of the original intensity, respectively, indicating acceptable selectivity of this biosensor.
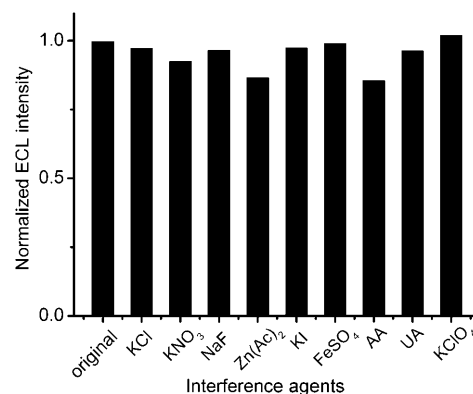


Figure 8. Normalized ECL intensities of the ECL biosensor in the air-saturated detection solution containing 5 μM of HQ with 10 μM of the individual interference agent.

**Stability, precision, and reproducibility of the biosensor**: Ten measurements of ECL emission upon continuous cyclic scans of GCE/QDs/chitosan (Figure 9A) and the GCE/QDs/HRP–chitosan biosensor (Figure 9B) in an air-saturated detection solution showed coincident signals with relative standard deviations (RSDs) of 1.1 and 1.4 %, respectively,
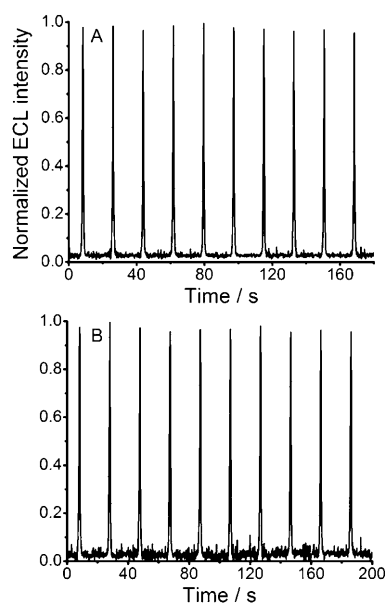


Figure 9. Continuous cyclic scans of A) GCE/QDs/chitosan and B) GCE/QDs/HRP–chitosan in an air-saturated detection solution.

indicating the reliability and stability of the signals. The RSD of five parallel measurements (intraassay) at 5 μM HQ with one biosensor was 4.3%, indicating a good precision. The ECL detection in presence of 5 μM HQ with five biosensors fabricated independently (interassay) showed the RSD of 3.4%, giving an acceptable fabrication reproducibility of the biosensor. When not in use, the biosensor was stored in 0.01 M pH 7.0 Tris-HCl buffer solution at 4 °C. After the biosensor was stored for 15 days, the ECL response for detection of 5 μM HQ did not show any evident decline when used once every five days, indicating acceptable storage stability.

## Conclusion

In this work we report on the synthesis of short-chain dithiol chelate CdTe QDs for forming surface traps, which successfully achieved the target to lower the band gap and the ECL emission potential of the QDs. The surface PL emission occurred at the same wavelength as the ECL emission. $H_2O_2$ formed from the reduction of dissolved oxygen was demonstrated to be a co-reactant of the cathodic ECL process, which avoided the presence of strong oxidants and made the ECL system much milder for bioanalysis. By co-immobilizing the as-prepared DMSA–CdTe QDs and HRP on a glassy carbon electrode, a new reagentless ECL biosensor for HQ, based on its quenching effect to the ECL emission, was obtained. The ECL quenching was due to the consumption of $H_2O_2$ in the enzymatic cycle. The biosensor showed an excellent performance. This work opens new avenues to the design of ECL emitters with low applied potential, demonstrated the extensive practicality of the surface-unpassivated QDs in ECL biosensing, and would be favorable to bioanalysis for a wide range of analytes.

## Experimental Section

**Materials and reagents**: Cadmium chloride ($CdCl_2·2.5H_2O$), DMSA, and HQ were purchased from Alfa Aesar China Ltd (China). HRP (EC 1.11.1.7, 250 U mg$^{-1}$ solid), chitosan (from crab shells), Tris-base (reagent grade) and MPA were purchased from Sigma Chemical Co. (MO, USA). Tellurium rod (4 mm in diameter) used as the Te electrode was purchased from Leshan Kayada Photoelectricity Co. (China). Other reagents were of analytical grade and used as received. 0.1 M pH 7.0 Tris-HCl buffer containing 0.1 M $KNO_3$ was used throughout the ECL detection and was defined as the detection solution. The air-free solution was obtained by bubbling highly pure $N_2$ to air-saturated detection solution for 20 min. Deionized water was used as the solvent throughout the work.

**Apparatus**: The electrochemical and ECL measurements were carried out on an MPI-E multifunctional electrochemical and chemiluminescent analytical system (Xi'an, China) at room temperature with a configuration that consisted of glassy carbon electrode (5 mm in diameter, China) as a working electrode, a platinum counter electrode and a Ag/AgCl (saturated KCl solution) reference electrode. The scan rate of the cathodic potential was 0.1 V s$^{-1}$. The emission window was placed in front of the photomultiplier tube biased at −600 V (for GCE/QDs/chitosan) or −800 V (for phenolic biosensor). The ECL spectrum was obtained by collecting the ECL data at −0.85 V during cyclic potential sweep with 11

filters (2 mm thickness) with transparent efficiency of around 88% at 650, 630, 600, 580, 550, 535, 510, 490, 470, 450, and 420 nm. PL and UV/Vis absorption spectra of the resulting solution of QDs were recorded on a RF-5301 PC fluorometer (Shimadzu Co., Japan) and a Shimadzu UV-3600 UV/Vis/NIR photospectrometer (Shimadzu Co., Japan), respectively. FT-IR spectra were recorded on Nicolet 400 FT-IR spectrometer (Madison, WI). The topography observation of QDs was carried out on a high-resolution transmission electron microscope (JEM-2100, JEOL). The impedance measurements were carried out on a PGSTAT30/FRA2 system (Autolab, Netherlands). The elemental analysis of DMSA–CdTe QDs and MPA–CdTe QDs were carried out on Elementar Vario MICRO (Germany). XPS experiments were performed on a K-Alpha X-ray photoelectron spectrometer (Thermo Fisher Scientific Co., USA) by using thoroughly dried QD powder, obtained by centrifugation of a solution of QDs and washed by 1:1 (v/v) mixture of deionized water and isopropyl alcohol, was used for the XPS experiment.

**Preparation of DMSA–CdTe and MPA–CdTe QDs**: The synthesis of DMSA–CdTe QDs was performed by using a "green method" with an electrogenerated precursor, which showed acceptable reproducibility. Briefly, an electrogenerated Te precursor for one-pot synthesis was produced on a CHI 660B workstation (Austin, TX) by using a Te electrode as a working electrode at −1.0 V (vs. Ag/AgCl) in the electrolyte containing 0.6 mM $Cd^{2+}$ and 1.6 mM DMSA as stabilizer under an $N_2$ atmosphere. The final quantity of electricity was 0.5 coulombs. After electrolysis, the solution was heated to reflux at 80 °C for 20 h to get the QD product. The final solution of QDs was stable for more than 2 months when kept in a refrigerator at 4 °C. The Te electrode could be recycled by polishing on a 1200 grit sand paper (Shanghai, China). The synthesis of the MPA–CdTe QDs performed under the same conditions, and the stabilizer was used in a large excess.

**Construction of GCE/QDs/chitosan and GCE/QDs/HRP–chitosan ECL biosensor**: The GCE was polished successively with 0.3 and 0.05 μm alumina slurry (Beuhler), followed by rinsing thoroughly with deionized water. After successive sonication, the electrode was rinsed with deionized water and allowed to dry with a $N_2$ stream. Then, the as-prepared solution of QDs (300 μL) was mixed with of isopropyl alcohol (300 μL) and centrifuged at 6000 rmp min$^{-1}$ for 3 min. The precipitate was washed twice by using 1:1 (v/v) mixture of deionized water and isopropyl alcohol, and then dissolved in deionized water (20 μL); the resulting solution was added dropwise to the polished GCE. After being dried in air, chitosan (0.1%; 10 μL) or a mixture of HRP (10 μL of 3 U μL$^{-1}$) and chitosan (0.5%; 10 μL) was covered over the QD film to obtain a stable GCE/QDs/chitosan or ECL biosensor (GCE/QDs/HRP–chitosan). The latter was dried at 4 °C and stored in 0.01 M pH 7.0 Tris-HCl buffer solution at 4 °C when not in use. The GCE/QDs/chitosan maintained similar ECL peak shape and ECL emission intensity after exposed to air for one month.

[1] M. M. Richter, *Chem. Rev.* **2004**, *104*, 3003.

[2] W. J. Miao, *Chem. Rev.* **2008**, *108*, 2506.

[3] S. Stagni, A. Palazzi, S. Zacchini, B. Ballarin, C. Bruno, M. Marcaccio, F. Paolucci, M. Monari, M. Carano, A. J. Bard, *Inorg. Chem.* **2006**, *45*, 695.

[4] M. Zhou, G. P. Robertson, J. Roovers, *Inorg. Chem.* **2005**, *44*, 8317.

[5] W. Zhan, A. J. Bard, *Anal. Chem.* **2007**, *79*, 459.

[6] X. Yang, R. Yuan, Y. Q. Chai, Y. Zhuo, L. Mao, S. R. Yuan, *Biosens. Bioelectron.* **2010**, *25*, 1851.

[7] L. Z. Hu, Z. Bian, H. J. Li, S. Han, Y. L. Yuan, L. X. Gao, G. B. Xu, *Anal. Chem.* **2009**, *81*, 9807.

[8] X. F. Wang, Y. Zhou, J. J. Xu, H. Y. Chen, *Adv. Funct. Mater.* **2009**, *19*, 1444.

[9] H. Jiang, H. X. Ju, *Anal. Chem.* **2007**, *79*, 6690.

[10] X. Liu, H. X. Ju, *Anal. Chem.* **2008**, *80*, 5377.

[11] Z. F. Ding, B. M. Quinn, S. K. Haram, L. E. Pell, B. A. Korgel, A. J. Bard, *Science* **2002**, *296*, 1293.

[12] G. F. Jie, H. P. Huang, X. L. Sun, J. J. Zhu, *Biosens. Bioelectron.* **2008**, *23*, 1896.

[13] L. H. Zhang, X. Q. Zou, E. B. Ying, S. J. Dong, *J. Phys. Chem. C* **2008**, *112*, 4451.

[14] X. Liu, H. Jiang, J. P. Lei, H. X. Ju, *Anal. Chem.* **2007**, *79*, 8055.

[15] H. Jiang, H. X. Ju, *Chem. Commun.* **2007**, 404.

[16] F. Li, Y. B. Zu, *Anal. Chem.* **2004**, *76*, 1768.

[17] X. Liu, L. Guo, L. X. Cheng, H. X. Ju, *Talanta* **2009**, *78*, 691.

[18] Y. Xing, Q. Chaudry, C. Shen, K. Y. Kong, H. E. Zhau, L. W. Chung, J. A. Petros, R. M. O'Regan, M. V. Yezhelyev, J. W. Simons, M. D. Wang, S. Nie, *Nat. Protoc.* **2007**, *2*, 1152.

[19] O. T. Bruns, H. Ittrich, K. Peldschus, M. G. Kaul, U. I. Tromsdorf, J. Lauterwasser, M. S. Nikolic, B. Mollwitz, M. Merkel, N. C. Bigall, S. Sapra, R. Reimer, H. Hohenberg, H. Weller, A. Eychmüller, G. Adam, U. Beisiegel, J. Heeren, *Nat. Nanotechnol.* **2009**, *4*, 193.

[20] X. Michalet, F. F. Pinaud, L. A. Bentolila, J. M. Tsay, S. Doose, J. J. Li, G. Sundaresan, A. M. Wu, S. S. Gambhir, S. Weiss, *Science* **2005**, *307*, 538.

[21] R. Freeman, R. Gill, I. Shweky, M. Kotler, U. Banin, I. Willner, *Angew. Chem.* **2009**, *121*, 315; *Angew. Chem. Int. Ed.* **2009**, *48*, 309.

[22] R. Gill, M. Zayats, I. Willner, *Angew. Chem.* **2008**, *120*, 7714; *Angew. Chem. Int. Ed.* **2008**, *47*, 7602.

[23] N. Myung, Y. Bae, A. J. Bard, *Nano Lett.* **2003**, *3*, 1053.

[24] S. K. Poznyak, N. P. Osipovich, A. Shavel, D. V. Talapin, M. Y. Gao, A. Eychmüller, N. Gaponik, *J. Phys. Chem. B* **2005**, *109*, 1094.

[25] C. W. Ge, M. Xu, J. Liu, J. P. Lei, H. X. Ju, *Chem. Commun.* **2008**, 450.

[26] H. T. Uyeda, I. L. Medintz, J. K. Jaiswal, S. M. Simon, H. Mattoussi, *J. Am. Chem. Soc.* **2005**, *127*, 3870.

[27] H. Borchert, D. V. Talapin, N. Gaponik, C. McGinley, S. Adam, A. Lobo, T. Möller, H. Weller, *J. Phys. Chem. A* **2003**, *107*, 9662.

[28] W. W. Yu, L. H. Qu, W. Z. Guo, X. G. Peng, *Chem. Mater.* **2003**, *15*, 2854.

[29] Z. T. Deng, O. Schulz, S. Lin, B. Q. Ding, X. W. Liu, X. X. Wei, R. Ros, H. Yan, Y. Liu, *J. Am. Chem. Soc.* **2010**, *132*, 5592.

[30] S. L. Zhao, Y. Huang, R. J. Liu, M. Shi, Y. M. Liu, *Chem. Eur. J.* **2010**, *16*, 6142.

[31] K. Iwasaki, T. Torimoto, T. Shibayama, H. Takahashi, B. Ohtani, *J. Phys. Chem. B* **2004**, *108*, 11946.

[32] Y. Bae, N. Myung, A. J. Bard, *Nano Lett.* **2004**, *4*, 1153.

[33] Y. M. Fang, J. J. Sun, A. H. Wu, X. L. Su, G. N. Chen, *Langmuir* **2009**, *25*, 555.

[34] Y. Shan, J. J. Xu, H. Y. Chen, *Chem. Commun.* **2009**, 905.

[35] A. J. S. Ahammad, S. Sarker, M. A. Rahman, J. J. Lee, *Electroanalysis* **2010**, *22*, 694.

[36] W. J. Dong, C. Dong, S. M. Shuang, M. M. F. Choi, *Biosens. Bioelectron.* **2010**, *25*, 1043.

[37] A. S. Santos, A. C. Pereira, M. D. P. T. Sotomayor, C. R. T. Tarley, N. Durán, L. T. Kubota, *Electroanalysis* **2007**, *19*, 549.

[38] S. K. Ozoner, E. Erhan, F. Yilmaz, A. Celik, B. Keskinler, *Talanta* **2010**, *81*, 82.

[39] S. Korkut, B. Keskinler, E. Erhan, *Talanta* **2008**, *76*, 1147.

[40] J. P. Yuan, W. W. Guo, E. K. Wang, *Anal. Chem.* **2008**, *80*, 1141.